

# Microcanonical calculations of excess thermodynamic properties of dense binary systems

Christophe Winisdoerffer\* and Gilles Chabrier†  
*École normale supérieure de Lyon, CRAL (UMR  
CNRS No. 5574), 69364 Lyon Cedex 07, France*

Gilles Zérah‡  
*Commissariat à l'Énergie Atomique,  
BP 12, 91680 Bruyères-le-Châtel, France*

(Dated: November 17, 2018)

## Abstract

We derive a new formulation to calculate the excess chemical potential of a fraction of  $N_1$  particles interacting with  $N_2$  particles of a different species. The excess chemical potential is calculated numerically from first principles by coupling molecular dynamics and Thomas-Fermi density functional theory to take into account the contribution arising from the quantum electrons on the forces acting on the ions. The choice of this simple functional is motivated by the fact that the present paper is devoted to the derivation and the validation of the method but more complicated functionals can and will be implemented in the future. This new method is applied in the microcanonical ensemble, the most natural ensemble for molecular dynamics simulations. This avoids the introduction of a thermostat in the simulation, and thus uncontrolled modifications of the trajectories calculated from the forces between particles. The calculations are conducted for three values of the input thermodynamic quantities, energy and density, and for different total numbers of particles in order to examine the uncertainties due to finite size effects. This method and these calculations lie the basic foundation to study the thermodynamic stability of dense mixtures, without any *a priori* assumption on the degree of ionization of the different species.

PACS numbers: 52.25.-b, 52.27.Gr, 52.65.-y

---

\*Electronic address: cwinisdo@ens-lyon.fr

†Electronic address: chabrier@ens-lyon.fr

‡Electronic address: zerah@cea.fr

## I. INTRODUCTION

The thermodynamic stability of dense ionic mixtures bears important consequences not only on our understanding of the thermodynamic properties of dense binary systems but also on the structure and the evolution of gaseous giant planets. Indeed, the interior of jovian planets is composed essentially of hydrogen and helium under either atomic or molecular form in the outermost envelope and under the form of a partially or fully ionized plasma in the inner regions [1] [2]. Temperatures and pressures along the Jupiter or Saturn internal isentrope conditions range from about 100 K to  $\sim 20000$  K and from about 1 bar to  $\sim 60$  Mbar. Under these conditions, not only the hydrogen/helium mixture experiences pressure ionization but the homogeneous mixture may become thermodynamically unstable. Such an immiscibility between helium-rich droplets and a hydrogen-rich fluid will liberate extra gravitational energy, modifying significantly the energy balance and thus the cooling of the planet [3] [4] [5]. For terrestrial applications, inertial confinement fusion experiments or laser-driven shock-wave experiments on hydrogen isotopes reach densities and temperatures characteristic of the aforementioned planetary conditions, probing the thermodynamic properties of dense plasmas and requiring a correct theoretical foundation to describe their equilibrium properties.

The theoretical description of the thermodynamic phase diagram of a dense two-component system is a particularly complicated task, for it requires a correct description of the *excess* free enthalpy (in a pressure-temperature diagram) of the mixture with respect to the pure phases. This excess quantity is very small compared with the contributions of both the mixture and the pure phases (it is by definition close to zero near the critical point) and therefore must be calculated with very high accuracy. Early calculations, based on simplified analytic or semi-analytic calculations of the free energy of the plasma, assumed hydrogen and helium atoms to be fully ionized [6] [7] [8] [9]. Moreover, these calculations assumed either a rigid electron background, the so-called binary ionic mixture (BIM) model, or a polarizable electron background within the linear response approximation. Although correct at very high density or temperature, these assumptions fail when electrons and protons start to recombine. The phase diagrams calculated under these conditions are thus restricted to a reduced (high) density-temperature range. Further attempts to do a consistent, first-principle determination of the H/He phase diagram, with no assumption on the electron distribution

around the ionic centers and a correct treatment of the various  $N$ -body ion and electron interactions, were based either on extrapolation at finite-temperature of zero-temperature calculations [10] or on incorrect thermodynamics integration [11] and thus remain also of doubtful validity. Under such circumstances, it is clear that not only the thermodynamic phase diagram of a hydrogen-helium system at high density has not been established accurately yet, but the correct calculation of the excess free enthalpy of a concentration of atoms immersed in an interacting system of different species remains to be done.

In this paper, we derive a new method to address this very point, which is crucial for a reliable determination of the thermodynamic phase diagram of dense binary mixtures. This method is applied in the microcanonical ensemble and allows the direct calculation, from first principles, of the excess chemical potential of a binary mixture of nuclei and electrons interacting through the Coulomb potential. Calculations in the microcanonical ensemble allow a fully consistent calculation between the forces acting on the particles and the induced trajectories, without the introduction of thermostats. We first derive the thermodynamic equations which allow the exact determination of the excess chemical potential. We then combine the density functional theory (DFT) to describe the quantum mechanical properties of the electrons and molecular dynamics (MD) to integrate the ion classical equations of motion to calculate this chemical potential. Since the present paper is devoted to the derivation of the method, we use a simplified functional form for the electrons, namely the Thomas-Fermi approximation, in order to speed up the minimization of the energy. We limit our calculations to three different values of the appropriate input thermodynamic quantities, namely energy and density in the microcanonical formulation used in the present paper. In a future work, devoted to the global analysis of the H/He mixture under various thermodynamic conditions, a more general functional form will be implemented. Section 2 presents the derivation of the chemical potential of  $N_1$  atoms of a given species interacting with  $N_2$  nuclei of a different species. Section 3 describes our general energy functional to take into account the quantum behaviour of the electrons when computing the ionic configurations, a necessary condition for an accurate treatment of the problem. Section 4 is devoted to the description of the MD numerical computations, to the discussion of the finite size effects and to the presentation of the results obtained for different thermodynamic conditions. The last section is devoted to the conclusion.

## II. DERIVATION OF THE EXCESS CHEMICAL POTENTIAL

As mentioned in the introduction, the ultimate goal of our calculations is to determine the thermodynamic stability of a given number  $N_1$  of atoms immersed in a system of  $N_2$  particles of a different species under given thermodynamic conditions, without any assumption on the electron distribution around the nuclei, *i.e.* on the degree of ionization of the atoms. The stability of such a mixture involves the calculation of the mixing enthalpy of the system, *i.e.* of the excess chemical potential of each immersed atom. The chemical potential  $\mu_i$  of a particle  $i$  immersed in a plasma corresponds by definition to the change of the state function of the appropriate thermodynamic ensemble when one adds or removes this particle to/from the plasma. When the thermodynamic limit is achieved ( $N \rightarrow \infty, V \rightarrow \infty, N/V = \text{constant}$ ), the result does not depend either on the ensemble or on the fact that the particle has been added to or removed from the surrounding plasma. Because of the large fluctuations of the system away from its equilibrium configuration, one can not add or remove directly a particle, in particular at high density or if the interaction potential is too stiff. The correct approach consists in modifying progressively the interaction potential  $\lambda V(r)$  between the particle  $i$  and the surrounding particles  $j \neq i$ . The case  $\lambda = 0$  corresponds to the case where the particle  $i$  does not interact with the other particles, but retains its discernability character (case of an ideal mixture), whereas the case  $\lambda = 1$  corresponds to the sought two-component system with full interactions. This method illustrates the so-called thermodynamic integration approach. In the microcanonical ensemble, with fixed energy, volume and number of particles ( $E, \mathcal{V}, N$ ), the chemical potential of a particle “1” of mass  $m_1$  corresponds to the calculation of the following expression derived in appendix A-C:

$$\begin{aligned}
 -\frac{\mu_1}{kT} = & \ln \left[ \left( \frac{2\pi m_1}{h^2} \right)^{3/2} \left( \frac{\sum_{j=1}^N m_j}{\sum_{j=1}^{N+1} m_j} \right)^{3/2} \frac{1}{N_1 + 1} \frac{\Gamma\left(\frac{3(N-1)}{2}\right)}{\Gamma\left(\frac{3N}{2}\right)} \mathcal{V} \langle K_N^{\frac{3}{2}} \rangle \right] \\
 & + \left( \frac{3N}{2} - 1 \right) \int_{\lambda=0}^{\lambda=1} d\lambda \left\langle \frac{1}{E(\lambda) - V} \frac{\partial E(\lambda)}{\partial \lambda} \right\rangle, \tag{1}
 \end{aligned}$$

where  $\Gamma$  is the Gamma function,  $\mathcal{V}$  is the cell volume,  $K_N$  is the kinetic energy and  $E(\lambda)$  is the energy corresponding to the system with the interaction potential  $\lambda V(r)$ . The brackets  $\langle \dots \rangle$  denote a microcanonical average. The first term on the right hand side is the ideal part of the chemical potential, arising from the entropy cost due to the particle insertion

or removal, while the second term represents the non-ideal contribution of the chemical potential, which depends on the interaction between the particle under consideration and the rest of the system. The integral can be estimated by a Gauss-Legendre quadrature [12]:

$$\int_{\lambda=0}^{\lambda=1} d\lambda \left\langle \frac{1}{E(\lambda) - V} \frac{\partial E(\lambda)}{\partial \lambda} \right\rangle \simeq \frac{1}{2} \sum_{i=1}^n \omega_i \left\langle \frac{1}{E(\lambda) - V} \frac{\partial E(\lambda)}{\partial \lambda} \right\rangle_{\lambda_i = \frac{x_i + 1}{2}}, \quad (2)$$

where  $x_i$  are the zeros of Legendre polynomials and  $\omega_i$  are the associated weights [13].

These calculations, in practice, require great caution. By definition of the microcanonical ensemble, the total (potential+kinetic) energy of the system must be conserved along the simulation. As a consequence, at each step where the potential goes from  $\lambda_i V$  to  $\lambda_{i+1} V$ , the kinetic part of the energy must be renormalized in order to maintain the total energy constant. Therefore, the correct calculation of the chemical potential consists in generating several particle configurations (to be described in §4) corresponding to the Hamiltonian  $H + \lambda V$ , and in computing the averages which appear in Eq.(1). This can be done by a fully classical simulation if the interaction between each kind of particles is described by a classical 2-body potential between particles. Such an approach, however, can not take into account the fact that the potentials strongly depend on the density and the temperature, evolving from a potential characteristic of atoms at low density and temperature to a long-range Coulomb potential characteristic of a fully ionized plasma at high density and/or temperature. Therefore, the correct phase diagram, without any assumption on the interaction potentials, requires *ab initio* generations of representative ionic configurations. This approach is presented in the next sections.

### III. THE FUNCTIONAL OF THE ELECTRONS

As mentioned in the introduction, a correct study of the problem under consideration requires a correct treatment of the ion and electron interactions. This implies to take into account the effects of the quantum nature of the electrons on the forces acting on the ions. Since the pioneering work of Hohenberg and Kohn [14], many problems involving interacting electrons have been tackled within the framework of the density functional theory (DFT). This theory turns the diagonalization problem of a many-body Hamiltonian into the minimization of a functional  $\Omega[n(\mathbf{r})]$  of the electron density, a much easier approach

when dealing with many electrons. For this reason, the DFT has been extensively used in condensed matter and is described in detail in many textbooks (see e.g. [15]). In the framework of the DFT, the grand potential of the electrons can be written in the form:

$$\Omega[n(\mathbf{r})] = \int d\mathbf{r} (V_{\text{ie}}(\mathbf{r}) - \mu) n(\mathbf{r}) + F[n(\mathbf{r})], \quad (3)$$

where  $F[n(\mathbf{r})]$  is a universal functional of the ground state density  $n(\mathbf{r})$  of the interacting electrons and  $V_{\text{ie}}(\mathbf{r})$  denotes the external ion-electron potential.  $\Omega[n(\mathbf{r})]$  is minimum when  $n(\mathbf{r})$  corresponds to the correct density. In our calculations, we have chosen to write  $\Omega[n(\mathbf{r})]$  under the following simplified form (in order to speed up the minimization):

$$\begin{aligned} \Omega[n(\mathbf{r})] = & k_B T \int d\mathbf{r} n(\mathbf{r}) \frac{F_{3/2}(\eta)}{F_{1/2}(\eta)} + c_{\text{ex}} \int d\mathbf{r} [n(\mathbf{r})]^{4/3} + E_{\text{corr}}[n(\mathbf{r})] \\ & + c_W \int d\mathbf{r} \frac{[\nabla n(\mathbf{r})]^2}{n(\mathbf{r})} + \frac{e^2}{2} \iint d\mathbf{r}_1 d\mathbf{r}_2 \frac{n(\mathbf{r}_1)n(\mathbf{r}_2)}{|\mathbf{r}_1 - \mathbf{r}_2|} \\ & + \int d\mathbf{r} n(\mathbf{r}) (V_{\text{ie}}(\mathbf{r}, \mathbf{R}_{\text{ion}}) - \mu), \end{aligned} \quad (4)$$

where  $c_{\text{ex}} = -\frac{3}{4}(3/\pi)^{1/3}e^2$  is the exchange Dirac coefficient,  $c_W = (\sigma/8)\hbar^2/m_e$  is the von Weizsäcker gradient correction coefficient [15] [16] (with  $\sigma = 1$  in our case), and  $E_{\text{corr}}[n(\mathbf{r})]$  is given by a parametrization [17] of Monte Carlo simulations [18].  $F_{3/2}(\eta)$  and  $F_{1/2}(\eta)$  are the Fermi integrals, where  $\eta = (\mu - V(\mathbf{r}))/k_B T$  is obtained by the inversion of the relation:  $n(\mathbf{r}) = (2\pi^2)^{-1}(2m_e/\hbar^2)^{3/2}(k_B T)^{3/2}F_{1/2}(\eta)$ . Accurate fitting formulae of the Fermi integrals and inverse integrals have been published in the literature [19] [20]. For a given configuration of the nuclei, we are able to find the electronic density  $n(\mathbf{r})$  which corresponds to the ground state of the system. The Hellmann-Feynman theorem [21] [22] enables us to calculate the forces arising from this electron density acting on the nuclei and the stress tensor on a cell (of which diagonal terms correspond to the pressure components).

Within the Born-Oppenheimer approximation, we can thus make a classical molecular dynamics (MD) simulation of the nuclei sub-system, while taking into account in the calculation of the forces the quantum behaviour of the electrons. The Born-Oppenheimer approximation expresses the fact that the electrons respond instantaneously to a change of configuration of the ions, a fairly good assumption for dense ionic systems. The calculation of the last term on the right hand side of Eq.(4), *i.e.* the interaction with the external ionic potential, involving effective pseudopotentials, is described below.

## IV. MOLECULAR DYNAMICS

### A. Method

We have computed Eq.(1) for a number of  $N_1$  helium atoms of nuclear charge  $Z_1 = 2$  and mass  $M_1$  immersed in a system of  $N_2$  hydrogen particles of charge  $Z_2 = 1$  and mass  $M_2$ . The thermodynamic averages in Eq.(1) are estimated by generating a set of representative configurations of the system in a cubic reference cell of size  $L$  with periodic boundary conditions. This is done by a dynamical simulation of the equations of motion for the ions:

$$M_i \frac{d^2 \mathbf{R}_i}{dt^2} = \mathbf{F}_i, \quad (5)$$

where  $M_i$  is the mass of the  $i$ th nuclei. The forces  $\mathbf{F}_i$  between particles (or equivalently the total potential  $V(\mathbf{r})$ ) arising from electron and ion  $N$ -body interactions, beyond any linear approximation for the electron-induced screening effects of the core potential, are calculated from a density functional approach. These forces involve the ones arising from the quantum electron distribution obtained from Eq.(4) and the ones derived from the interionic potential  $Z_i Z_j e^2 / |\mathbf{R}_i - \mathbf{R}_j|$ . The equations of motion are solved with a standard Verlet velocity algorithm [23]. The crucial point of the present paper is that these calculations are completed in the microcanonical ensemble, *i.e.* at constant energy, volume and total momentum [24]. Standard simulations, in other thermodynamic ensembles, imply the introduction of a thermostat, either by reinitializing the velocities “periodically” or by introducing new degrees of freedom. These thermostats, however, yield a perturbation of the trajectories, which no longer represent the ones determined by the forces. Such unphysical effects are avoided in the present microcanonical calculations, which insure full consistency between the forces and the trajectories.

The *ab initio* calculations, with the aforescribed functional, have been performed with the ABINIT code [25]. We replace the bare Coulomb potential of the nucleus by a pseudopotential, which differs from the true Coulomb potential below a cutoff radius  $r_{\text{loc}}$ , removing the cusp constraint at  $r \rightarrow 0$  and avoiding the  $1/r$  singularity. The pseudopotentials used in our simulations are those of Hartwigsen *et al.* for helium [26], and Goedecker *et al.* for hydrogen [27]. These pseudopotentials are constructed so as to reproduce with high accuracy the Kohn-Sham free energy.

The aforementioned cutoff radius determines an upper bound in density for the domain of validity of the pseudopotentials. The ones used in the present calculations [28] have  $r_{\text{loc}} = 0.2$  bohr, which implies a density limit:  $a \gtrsim r_{\text{loc}}$ , *i.e.*  $r_s \gtrsim 0.2$ , where  $r_s = a/a_0$  is the density parameter,  $a = (\frac{V}{4\pi N/3})^{1/3}$  is the mean distance between nuclei and  $a_0$  is the Bohr radius. This condition corresponds to  $\rho \lesssim 335 \text{ g cm}^{-3}$ .

As mentioned earlier, in order to maintain the total energy constant during the process of switching on or off the interaction, the kinetic contribution  $E_{\text{kin}}$  must be renormalized. For the thermodynamic conditions of our runs, this corresponds to a decrease of  $E_{\text{kin}}$  because the potential energy increases as the interaction is switched on ( $\lambda = 0 \rightarrow 1$ ). This implies a large initial kinetic energy. The condition is more easily fulfilled if one chooses to switch *off* the interaction instead of switching it on ( $\lambda = 1 \rightarrow 0$ ). Indeed, during such a process, the kinetic part must be increased (instead of decreased), which is always possible. As a consequence of this renormalization, we can not associate an accurate temperature until the thermodynamic limit is reached. This process is represented on Figure 1, which displays the kinetic energy during the whole process, and shows the discontinuities appearing in the mean value of  $E_{\text{kin}}$  when  $\lambda$  changes from  $\lambda_i$  to  $\lambda_{i+1}$ .

## B. Results

We have tested our procedure on a system consisting of 63 hydrogen nuclei and 1 helium nucleus. The thermodynamic conditions of our microcanonical simulation are:  $E_{\text{tot}} = 132.21$  hartree and  $V = L^3 = 57.906 \text{ bohr}^3$ , which correspond to  $r_s \simeq 0.6$ ,  $T \simeq 2 \cdot 10^5 \text{ K}$  and  $P \simeq 7 \cdot 10^4 \text{ GPa}$ . The reference cell of the simulation assumes periodic boundary conditions, with one particle exiting the cell on one side replaced by one entering the opposite side. In order for the final results not to depend on the initial distribution, which corresponds to a random distribution of the positions and velocities (obtained by a classical molecular dynamics simulation to prevent atoms to overlap), we let the system relax during 4000 time steps, a very conservative limit for the considered densities and temperatures. Even though the main contribution to the total energy at  $r_s = 0.6$  comes from the nearly uniform electron background, the forces depend partly on the non-uniformity of this electron density distribution. Therefore, in order to calculate the forces correctly, the electronic density, more precisely the departure of the density from a homogeneous distribution, must be calculated



with very high accuracy. In order to fulfil this condition, we require the energy to converge within  $|\Delta E/E| < 10^{-8}$ . Unfortunately, high accuracy in the functional minimization does not preclude energy fluctuations during the simulation due to the discretization of the Newton equations and, most importantly, to finite-size effects. These points are examined below. The equations of motion are solved using the Verlet algorithm with a time step equal to  $dt_{ion} = 0.25$  a.u. This time step enables us to resolve the dynamics of our system accurately for any value  $\lambda V$  of the He-H interaction. Figure 2 displays the conservation of the total energy obtained in our simulation with this time step. The integral Eq.(2) is first calculated with a  $M$ -point Gauss-Legendre quadrature. After the first 4000 time steps to let the system relax, an other 4000 time steps simulation is ran to generate several configurations. The argument  $\partial_\lambda E(\lambda)/(E(\lambda) - V)$  is calculated numerically, by calculating  $E(\lambda \pm 0.01)$  every 10 time steps for a fixed configuration and  $E(\lambda) - V$ . A last run is devoted to the calculations of the ideal part of the chemical potential by generating 10000 different configurations of 63 H and the evaluation of  $\langle K_N^{3/2} \rangle$ .

We have tested the validity of the  $M$ -point quadrature to estimate the integral Eq.(2) by doing similar calculations, for the same thermodynamic conditions, with a 3-point, 6-point and a 9-point quadrature. The results are shown on Figure 3, and the resulting evaluations of the integral are given in Table I. As seen in this table, a 6-point quadrature is enough to calculate accurately the integral (2). Our calculations of the chemical potential  $-\frac{\mu_1}{kT}$  of a helium atom embedded in a 63-H plasma for our thermodynamic conditions ( $-\frac{\mu_1^0}{kT}$  corresponds to the ideal part of the chemical potential and  $-\frac{\mu_1^1}{kT}$  to the excess contribution) yield:

$$\left\{ \begin{array}{l} -\frac{\mu_1^0}{kT} = 14.02, \\ -\frac{\mu_1^1}{kT} = 5.14, \\ -\frac{\mu_1}{kT} = 19.16. \end{array} \right. \quad (6)$$

In order to estimate the  $N$ -dependence of our result, we have also calculated the entropy cost which corresponds to the removal of 2 He-particles surrounded by 126 H, and 4 He-particles surrounded by 252 H, for the same thermodynamic conditions (density and energy) as for the {1 He, 63 H} system. These computations are much more time consuming (the

computation time scales roughly as  $t \propto N^3$ ), and the removal of the helium atom must be done 2 and 4 times, respectively. We expect a very small dependence of the results on the size ( $N$ ) of the simulated system. Indeed, we do not calculate the chemical potential of *one* He atom but the chemical potential of a constant *fraction* ( $x_{\text{He}}=1/64$ ) of He in a H-He mixture. As a consequence, the  $N$ -dependence of the results stems from the interaction between a He atom with its replicas (due to the periodic condition boundaries) and from the fact that the accessible phase space increases with the total number of atoms. The first effect becomes important when the characteristic length of interaction is of the same order as the simulated box, *i.e.* at much higher density than the present simulations. Quantification of the second effect requires simulations with different values of  $N$ . The results are presented in Table II. The chemical potential is estimated with a centered scheme, *i.e.* the chemical potential corresponding to a Helium fraction  $x_{\text{He}}=1/128=0.008$  is evaluated from the entropy difference between the  $\{0 \text{ He}, 63 \text{ H}\}$  system and the  $\{1 \text{ He}, 63 \text{ H}\}$  system (with full interaction). The statistical uncertainties on  $-\mu_1/kT$  are  $\pm 0.02$  for the  $\{1 \text{ He}, 63 \text{ H}\}$  and  $\{2 \text{ He}, 126 \text{ H}\}$  systems, and  $\pm 0.04$  for the  $\{4 \text{ He}, 252 \text{ H}\}$  one (achieving the same statistical uncertainties scales as  $N^3$ ). The results between the three systems for a He fraction equal to 0.008, as shown in the Table, are thus fully compatible, and no statistically-significant trend appears. The same simulations yield also the estimation of the Helium chemical potential for different number fractions. All the results are given in Table II, and are compatible within the statistical uncertainties. For the  $\{1 \text{ He}, 63 \text{ H}\}$  mixture, we have also conducted calculations for two other thermodynamic conditions, displayed in Table III. As expected intuitively, it is easier to add an atom in a low density plasma than in a high density one (at constant total energy), or in a cold plasma than in a hot one (at constant density).

It is interesting to compare our results with the limit of rigid electronic background at high density for the binary ionic mixture, the so-called BIM limit [29] [30]. Our reference conditions,  $E_{\text{tot}} = 132.21$  hartree and  $V = L^3 = 57.906$  bohr<sup>3</sup>, *i.e.*  $r_s \simeq 0.6$ , correspond to  $T = 2.2 \cdot 10^5$  K,  $P = 6.7 \cdot 10^4$  GPa and  $\Delta S = 19.15 k_B$  (Table II) in the simulation. For this density and temperature, the BIM corresponds to  $P = 7.2 \cdot 10^4$  GPa and  $\Delta S = 21 k_B$ . We have also ran a simulation at higher density, namely  $r_s = 0.3$ , which is close to the density limit of our pseudopotentials. The total energy is equal to  $E_{\text{tot}} = 672.76$  hartree. In that case, the present calculations yield  $T = 4.5 \cdot 10^5$  K,  $P = 2.15 \cdot 10^6$  GPa, whereas the BIM results are  $T = 4.5 \cdot 10^5$  K,  $P = 2.2 \cdot 10^6$  GPa. The small differences between the simulations

TABLE I: Integration of Equation 2.

	3 points	6 points	9 points	trapeze
$\int_{\lambda=0}^{\lambda=1} d\lambda \left\langle \frac{1}{E(\lambda) - V} \frac{\partial E(\lambda)}{\partial \lambda} \right\rangle$	0.06568	0.05578	0.05548	0.05565

TABLE II: Finite size effects on the chemical potential.

System	{1 He, 63 H}			{2 He, 126 H}			{4 He, 252 H}		
$x_{\text{He}} = N_{\text{He}}/(N_{\text{H}} + N_{\text{He}})$	0.004	0.008	0.012	0.004	0.008	0.012	0.004	0.008	0.012
$-\frac{\mu_1}{kT}$	x	19.16	x	19.15	19.15	19.15	19.17	19.14	19.21

and the BIM reflect the contribution due to the electron gas polarization (inhomogeneous distribution), which starts playing a role around these densities, and the contribution due to the interactions between particles of *different species* (namely H and He). These latter are not taken into account in the BIM, which is based on the so-called linear volume law, where only the ideal entropy of mixture is included.

## V. CONCLUSION

In this paper, we have derived a new method, based on physics first principles, to calculate the excess potential of a number fraction of particles immersed in a mixture of particles of different species, as given by Eq.(1). The calculations are based on a consistent treatment of the forces acting on the nuclei, taking into account the contribution arising from the quantum electrons, by calculating self-consistently the equations of motion of the classical nuclei and the functional density of the electronic distribution. The method is applied directly in the microcanonical ensemble, avoiding the use of a thermostat, and thus insures consistency

TABLE III: Chemical potentials for different thermodynamic conditions.

$\{E_{\text{tot}}(\text{hartree}), V(\text{bohr}^3)\}$	{132.21,57.91}	{132.21,139.40}	{20.06,139.40}
$r_s$	0.6	0.8	0.8
$-\frac{\mu_1}{kT}$	19.16	16.59	13.94

between the forces and the trajectories of the particles. The bare Coulomb potential is approximated at short distances by pseudopotentials which remain valid up to large densities ( $r_s \gtrsim 0.2$ ), where the linear response theory becomes valid. The thermodynamic quantities are calculated for different configurations, representing the evolution of the interaction, and thus of the system, from the initial case of an *ideal* atom “1” inserted in a system of particles “2” to the final case where all interactions between the immersed particle and the surrounding nuclei are taken into account. Only properly following such a series of changes of equilibrium states insures thermodynamic consistency and thus allows a correct evaluation of the energy and pressure contributions to the excess chemical potential of the immersed particle. Previous simulations [11] calculated the excess enthalpy directly from the difference between the final and the initial states, yielding an incorrect evaluation of the contraction work, and thus of the pressure contribution.

The validity of the method has been tested with the case of a dense hydrogen/helium mixture for three different helium fractions and three different thermodynamic states. The forces are calculated with very high accuracy, with a convergence criterium  $|\Delta E/E| < 10^{-8}$ . Finite size effects on the final results have been quantified and found to be small ( $\sim 10^{-3}$ ) leading to fluctuations of the same order on the total energy (see Fig 2). The method provides robust foundations for accurate evaluations of the excess thermodynamic quantities of dense binary mixtures, without any assumption on the electron density distribution and thus on the degree of ionization of the atoms. This opens the door to accurate calculations of phase diagrams of dense mixtures of atoms and partially or fully ionized plasmas, a subject of prime interest for the structure and the evolution of giant gaseous planets. Work in this direction is in progress.

We are very grateful to Gérard Massacrier and Alexander Potekhin for very useful discussions and insightful remarks. We are also indebted to the two anonymous referees for their valuable comments which helped improving the initial manuscript.

## APPENDIX A: MICROCANONICAL AVERAGE

We consider a (classical) system with fixed total energy  $E$ , volume  $V$  and total momentum  $\mathbf{p}_{\text{tot}}$ , which contains two different kinds of particles,  $N_1$ ,  $N_2$ , with  $N = N_1 + N_2$ . In this

microcanonical ensemble, the number of accessible states for this system is:

$$\delta\Omega = \frac{\delta E}{h^{3N} N_1! N_2!} \int d\mathbf{p}^N d\mathbf{q}^N \delta(E - H) \delta(\mathbf{p}_{\text{tot}} - \sum_{j=1}^N \mathbf{p}_j), \quad (\text{A1})$$

where  $H = \sum_{j=1}^N \frac{\mathbf{p}_j^2}{2m_j} + V(\mathbf{q}^N)$  is the Hamiltonian of the ionic centers, and includes the modification of the Coulomb potentials due to the electron gas polarization,  $d\mathbf{p}^N = \prod_{i=1}^N \prod_{j=1}^3 dp_{ij}$ , and  $dp_{ij}$  is the  $j$ -component of the momentum of the particle  $i$ . Idem for  $d\mathbf{q}^N$ . Then:

$$\Omega = \frac{1}{h^{3N} N_1! N_2!} \int d\mathbf{p}^N d\mathbf{q}^N \theta(E - H) \delta(\mathbf{p}_{\text{tot}} - \sum_{j=1}^N \mathbf{p}_j) \equiv \frac{1}{h^{3N} N_1! N_2!} I(E, \mathbf{p}_{\text{tot}}), \quad (\text{A2})$$

where  $\theta(x) = 1$  if  $x > 0$ , 0 otherwise, and  $I(E, \mathbf{p}_{\text{tot}})$  denotes the integral.

The Laplace transform (toward  $E$ ) of  $I$  is [31]:

$$\begin{aligned} \mathcal{L}[I] &= \int d\mathbf{p}^N d\mathbf{q}^N \delta(\mathbf{p}_{\text{tot}} - \sum_{j=1}^N \mathbf{p}_j) \int_{\min(H)}^{+\infty} dE \theta(E - H) e^{-sE} \\ &= \int d\mathbf{p}^N d\mathbf{q}^N \delta(\mathbf{p}_{\text{tot}} - \sum_{j=1}^N \mathbf{p}_j) \frac{1}{s} e^{-sH} \\ &= \int d\mathbf{p}^N \delta(\mathbf{p}_{\text{tot}} - \sum_{j=1}^N \mathbf{p}_j) e^{-s \sum_{j=1}^N \frac{\mathbf{p}_j^2}{2m_j}} \int d\mathbf{q}^N \frac{1}{s} e^{-sV(\mathbf{q}^N)}. \end{aligned}$$

The Hamiltonian  $H$  is general and does not have, in particular, to be positive, although it needs to have a lower limit. Note that with a change of variable  $\zeta = E - \min(H)$ , the integral  $\int_{\min(H)}^{+\infty}$  becomes  $\int_0^{+\infty}$ , and the results remain unchanged.

Then:

$$J_0 = \int d\mathbf{p}^N \delta(\mathbf{p}_{\text{tot}} - \sum_{j=1}^N \mathbf{p}_j) e^{-s \sum_{j=1}^N \frac{\mathbf{p}_j^2}{2m_j}} \equiv J^3,$$

where  $J = \int dp_x^N \delta(p_{totx} - \sum_{j=1}^N p_{jx}) e^{-s \sum_{j=1}^N \frac{p_{jx}^2}{2m_j}}$ .

$J$  can be calculated by Fourier transformation:

$$\begin{aligned} \mathcal{F}[J] &= \int dp_x^N \frac{1}{\sqrt{2\pi}} \int_{-\infty}^{+\infty} dp_{totx} \delta(p_{totx} - \sum_{j=1}^N p_{jx}) \exp\left(-s \sum_{j=1}^N \frac{p_{jx}^2}{2m_j}\right) \exp(i\zeta p_{totx}) \\ &= \frac{1}{\sqrt{2\pi}} \prod_{j=1}^N \int dp_{jx} \exp\left(-s \frac{p_{jx}^2}{2m_j} + i\zeta p_{jx}\right) \\ &= \frac{1}{\sqrt{2\pi}} \left( \prod_{j=1}^N \sqrt{\frac{2\pi m_j}{s}} \right) \exp\left(-\frac{\sum_{j=1}^N m_j}{2s} \zeta^2\right). \end{aligned}$$

Then:

$$J = \mathcal{F}^{-1}[\mathcal{F}[J]] = \frac{\prod_{j=1}^N \sqrt{2\pi m_j}}{\sqrt{2\pi \sum_{j=1}^N m_j}} \frac{1}{s^{(N-1)/2}} \exp\left(-\frac{s}{2 \sum_{j=1}^N m_j} p_{totx}^2\right).$$

With  $\mathbf{p}_{tot} = 0$ , we get:

$$J_0 = J^3 = \left( \frac{\prod_{j=1}^N \sqrt{2\pi m_j}}{\sqrt{2\pi \sum_{j=1}^N m_j}} \right)^3 \frac{1}{s^{\frac{3(N-1)}{2}}},$$

and:

$$I = \mathcal{L}^{-1}[\mathcal{L}[I]] = \left( \frac{\prod_{j=1}^N \sqrt{2\pi m_j}}{\sqrt{2\pi \sum_{j=1}^N m_j}} \right)^3 \int d\mathbf{q}^N \theta(E - V(\mathbf{q}^N)) \frac{(E - V(\mathbf{q}^N))^{\frac{3(N-1)}{2}}}{\Gamma\left(\frac{3(N-1)}{2} + 1\right)}.$$

Equation (A2) thus reads:

$$\Omega(E, \mathbf{p}_{tot} = 0) = \frac{1}{h^{3N} N_1! N_2!} \left( \frac{\prod_{j=1}^N \sqrt{2\pi m_j}}{\sqrt{2\pi \sum_{j=1}^N m_j}} \right)^3 \int d\mathbf{q}^N \theta(E - V(\mathbf{q}^N)) \frac{(E - V(\mathbf{q}^N))^{\frac{3(N-1)}{2}}}{\Gamma\left(\frac{3(N-1)}{2} + 1\right)}. \quad (\text{A3})$$

In a similar way, we have for  $\omega \hat{=} \left(\frac{\partial \Omega}{\partial E}\right)_{V, N_1, N_2}$ :

$$\omega = \frac{1}{h^{3N} N_1! N_2!} \left( \frac{\prod_{j=1}^N \sqrt{2\pi m_j}}{\sqrt{2\pi \sum_{j=1}^N m_j}} \right)^3 \int d\mathbf{q}^N \theta(E - V(\mathbf{q}^N)) \frac{(E - V(\mathbf{q}^N))^{\frac{3(N-1)}{2} - 1}}{\Gamma\left(\frac{3(N-1)}{2}\right)}. \quad (\text{A4})$$

For a quantity depending only on  $\mathbf{q}^N$ , *i.e.*  $A(\mathbf{q}^N)$ , we have:

$$\begin{aligned} \langle A \rangle &\equiv \frac{1}{\omega} \frac{1}{h^{3N} N_1! N_2!} \int d\mathbf{p}^N d\mathbf{q}^N \delta(E - H) \delta(\mathbf{p}_{tot} - \sum_{j=1}^N \mathbf{p}_j) A(\mathbf{q}^N) \\ &= \frac{\int d\mathbf{q}^N \theta(E - V(\mathbf{q}^N)) (E - V(\mathbf{q}^N))^{\frac{3(N-1)}{2} - 1} A(\mathbf{q}^N)}{\int d\mathbf{q}^N \theta(E - V(\mathbf{q}^N)) (E - V(\mathbf{q}^N))^{\frac{3(N-1)}{2} - 1}}, \end{aligned} \quad (\text{A5})$$

where  $\langle \dots \rangle$  denotes a *microcanonical average*.

## APPENDIX B: CHEMICAL POTENTIAL BY THE PARTICLE INSERTION METHOD

The definition of the chemical potential of the particle 1 is:

$$-\frac{\mu_1}{kT} = \left( \frac{\partial S}{\partial N_1} \right)_{E, V, N_2}. \quad (\text{B1})$$

With  $S = k \ln \omega$  and the equations derived in Appendix A, this yields:

$$\begin{aligned} -\frac{\mu_1}{kT} &= \frac{\ln \omega_{N_1+1} - \ln \omega_{N_1}}{N_1 + 1 - N_1} = \ln \frac{\omega_{N_1+1}}{\omega_{N_1}} \\ &= \ln \left[ \left( \frac{2\pi m_1}{h^2} \right)^{3/2} \left( \frac{\sum_{j=1}^N m_j}{\sum_{j=1}^{N+1} m_j} \right)^{3/2} \frac{1}{N_1 + 1} \frac{\Gamma\left(\frac{3(N-1)}{2}\right)}{\Gamma\left(\frac{3N}{2}\right)} \frac{\int d\mathbf{q}^{N+1} \theta(E - V)(E - V(\mathbf{q}^{N+1}))^{\frac{3N}{2}-1}}{\int d\mathbf{q}^N \theta(E - V)(E - V(\mathbf{q}^N))^{\frac{3(N-1)}{2}-1}} \right]. \end{aligned} \quad (\text{B2})$$

Let define  $I_N$  as:

$$\begin{aligned} I_N &= \int d\mathbf{q}^N \theta(E - V(\mathbf{q}^N))(E - V(\mathbf{q}^N))^{\frac{3(N-1)}{2}-1} \\ &\equiv \int d\mathbf{q}^N \theta(E - V(\mathbf{q}^N)) K_N^{\frac{3(N-1)}{2}-1}, \end{aligned}$$

where  $K_N \equiv E - V(\mathbf{q}^N)$  is a function of  $\mathbf{q}^N$  and should not be formally confused with the kinetic part of the Hamiltonian (even if  $K_N$  is equal to the kinetic energy in a molecular dynamics simulation).

We get:

$$\begin{aligned} I_{N+1} &= \int d\mathbf{q}_{N+1} \int d\mathbf{q}^N \theta(E - V)(E - V(\mathbf{q}^N) - V(\mathbf{q}_{N+1}))^{\frac{3N}{2}-1} \\ &= \int d\mathbf{q}_{N+1} \int d\mathbf{q}^N \theta(E - V) K_N^{\frac{3}{2}} K_N^{\frac{3(N-1)}{2}-1} \left( 1 - \frac{V(\mathbf{q}_{N+1})}{K_N} \right)^{\frac{3N}{2}-1}, \end{aligned}$$

and:

$$\frac{I_{N+1}}{I_N} = \int d\mathbf{q}_{N+1} \left\langle K_N^{\frac{3}{2}} \left( 1 - \frac{V(\mathbf{q}_{N+1})}{K_N} \right)^{\frac{3N}{2}-1} \right\rangle,$$

which yields for the chemical potential:

$$-\frac{\mu_1}{kT} = \ln \left[ \left( \frac{2\pi m_1}{h^2} \right)^{3/2} \left( \frac{\sum_{j=1}^N m_j}{\sum_{j=1}^{N+1} m_j} \right)^{3/2} \frac{1}{N_1 + 1} \frac{\Gamma\left(\frac{3(N-1)}{2}\right)}{\Gamma\left(\frac{3N}{2}\right)} \int d\mathbf{q}_{N+1} \left\langle K_N^{\frac{3}{2}} \left( 1 - \frac{V(\mathbf{q}_{N+1})}{K_N} \right)^{\frac{3N}{2}-1} \right\rangle \right]. \quad (\text{B3})$$

## APPENDIX C: CHEMICAL POTENTIAL BY THE THERMODYNAMIC INTEGRATION METHOD

The variation of entropy when going from a state with interaction  $\lambda = 0$  to  $\lambda = 1$  reads:

$$\Delta S = \int_{\lambda=0}^{\lambda=1} d\lambda \frac{\partial S}{\partial \lambda}. \quad (\text{C1})$$

We can thus derive:

$$\begin{aligned} \frac{1}{k} \frac{\partial S}{\partial \lambda} &= \frac{1}{\omega} \frac{\partial \omega}{\partial \lambda} \\ &= \frac{\partial_\lambda \int d\mathbf{q}^{N+1} \theta(E(\lambda) - V(\mathbf{q}^{N+1})) (E(\lambda) - V(\mathbf{q}^{N+1}))^{\frac{3N}{2}-1}}{\int d\mathbf{q}^{N+1} \theta(E(\lambda) - V(\mathbf{q}^{N+1})) (E(\lambda) - V(\mathbf{q}^{N+1}))^{\frac{3N}{2}-1}} \\ &= \left( \frac{3N}{2} - 1 \right) \frac{\int d\mathbf{q}^{N+1} \theta(E(\lambda) - V(\mathbf{q}^{N+1})) \frac{1}{E-V} \frac{\partial E}{\partial \lambda} (E(\lambda) - V(\mathbf{q}^{N+1}))^{\frac{3N}{2}-1}}{\int d\mathbf{q}^{N+1} \theta(E(\lambda) - V(\mathbf{q}^{N+1})) (E(\lambda) - V(\mathbf{q}^{N+1}))^{\frac{3N}{2}-1}} \\ &= \left( \frac{3N}{2} - 1 \right) \left\langle \frac{1}{E-V} \frac{\partial E}{\partial \lambda} \right\rangle. \end{aligned}$$

The thermodynamic integration proceeds in two steps. The first one deals with the insertion of a free particle into the system. The entropy cost of this insertion is given by the formula established for the insertion method.

$$-\frac{\mu_1^0}{kT} = \ln \left[ \left( \frac{2\pi m_1}{h^2} \right)^{3/2} \left( \frac{\sum_{j=1}^N m_j}{\sum_{j=1}^{N+1} m_j} \right)^{3/2} \frac{1}{N_1 + 1} \frac{\Gamma\left(\frac{3(N-1)}{2}\right)}{\Gamma\left(\frac{3N}{2}\right)} \mathcal{V} \langle K_N^{\frac{3}{2}} \rangle \right], \quad (\text{C2})$$

where  $\mathcal{V}$  is the cell volume.

The interaction is then progressively switched on, and the non-ideal part of chemical potential is then given by:

$$-\frac{\mu_1^1}{kT} = \left( \frac{3N}{2} - 1 \right) \int_{\lambda=0}^{\lambda=1} d\lambda \left\langle \frac{1}{E(\lambda) - V} \frac{\partial E(\lambda)}{\partial \lambda} \right\rangle. \quad (\text{C3})$$

The total chemical potential is the sum of the two contributions:

$$-\frac{\mu_1}{kT} = -\frac{\mu_1^0}{kT} - \frac{\mu_1^1}{kT}. \quad (\text{C4})$$

[1] T. Guillot, G. Chabrier, D. Gautier and P. Morel, *Astrophys. J.* **450**, 463 (1995).

[2] W. Hubbard, A. Burrows and J. Lunine, *ARA&A* **40**, 103 (2002).



- [3] E. Salpeter, *Astrophys. J. Letters* **181**, L83 (1973).
- [4] D. Stevenson and E. Salpeter, *Astrophys. J. Supp.* **35**, 221 (1977).
- [5] D. Stevenson and E. Salpeter, *Astrophys. J. Supp.* **35**, 239 (1977).
- [6] D. Stevenson, *Phys. Rev. B* **12**, 3999 (1975).
- [7] J. Hansen, G. Torrie and P. Vieillefosse, *Phys. Rev. A* **16**, 2153 (1997).
- [8] P. Vieillefosse, *J. Phys.* **42**, 723 (1981).
- [9] G. Chabrier and T. Guillot (unpublished).
- [10] J. Klepeis, K. Schafer, T. Barbee and M. Ross, *Science* **254**, 986 (1991).
- [11] O. Pfaffenzeller, D. Hohl and P. Ballone, *Phys. Rev. Lett.* **74**, 2599 (1995).
- [12] W. Press, S. Teukolsky, W. Vetterling and B. Flannery, *Numerical recipes in FORTRAN. The art of scientific computing* (Cambridge University Press, 1987).
- [13] M. Abramowitz and I. Stegun, *Handbook of mathematical functions with formulas, graphs, and mathematical tables* (Dover, 1975).
- [14] P. Hohenberg and W. Kohn, *Phys. Rev.* **136**, B864 (1964).
- [15] R. Parr and W. Yang, *Density-Functional Theory of Atoms and Molecules* (Oxford University Press, 1989).
- [16] C. von Weizsäcker, *Z. Phys.* **96**, 431 (1935).
- [17] J. Perdew and Y. Wang, *Phys. Rev. B* **45**, 13244 (1992).
- [18] D. Ceperley and B. Alder, *Phys. Rev. Lett.* **45**, 566 (1980).
- [19] S. Blinnikov, N. Dunina-Barkovskaya and D. Nadyozhin, *Astrophys. J. Supp.* **106**, 171 (1996).
- [20] H. Antia, *Astrophys. J. Supp.* **84**, 101 (1993).
- [21] R. Feynman, *Phys. Rev.* **56**, 340 (1939).
- [22] O. Nielsen and R. Martin, *Phys. Rev. B* **32**, 3780 (1985).
- [23] D. Frenkel and B. Smit, *Understanding Molecular Simulation, From Algorithms to Application* (Academic Press, 1996).
- [24] In order to correct for numerical errors in the molecular dynamics simulation, it is convenient to fix also momentum, since the total momentum of the box must be conserved. In the thermodynamic limit, both ensembles lead to the same results.
- [25] ABINIT is a common project of the Université Catholique de Louvain, Corning Incorporated, and other contributors. Details can be found on the website <http://www.abinit.org>.
- [26] C. Hartwigsen, S. Goedecker and J. Hutter, *Phys. Rev. B* **58**, 3641 (1998).

- [27] S. Goedecker, M. Teter and J. Hutter, Phys. Rev. B **54**, 1703 (1996).
- [28] Even if atomic units are the most natural ones in the context of DFT, cgs ones may be more convenient in a different context; here are some conversion factors: 1 hartree  $\simeq 4.36 \cdot 10^{-11}$  erg, 1 bohr  $\simeq 0.53 \cdot 10^{-8}$  cm, and 1 atomic unit of time  $\simeq 2.42 \cdot 10^{-17}$  s.
- [29] G. Chabrier and A. Potekhin, Phys. Rev. E **58**, 4941 (1998).
- [30] A. Potekhin and G. Chabrier, Phys. Rev. E **62**, 8554 (2000).
- [31] The function  $I(x)$  is continuous by steps and is bound by  $\exp(ax)$  for  $x \rightarrow +\infty$  so that the Lapace transform can be applied to  $I(x)$ .

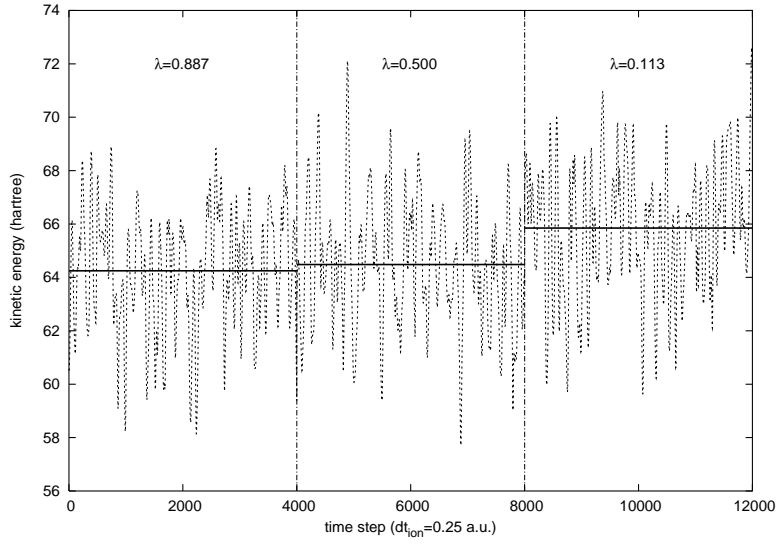


FIG. 1: Kinetic energy during the whole switch off of the helium atom embedded in a 63 hydrogen system, in the 3-point quadrature case. The average kinetic energies are displayed in solid line, the instantaneous ones into dashed line. The vertical lines separate the different domains of constant switching parameter  $\lambda$ .

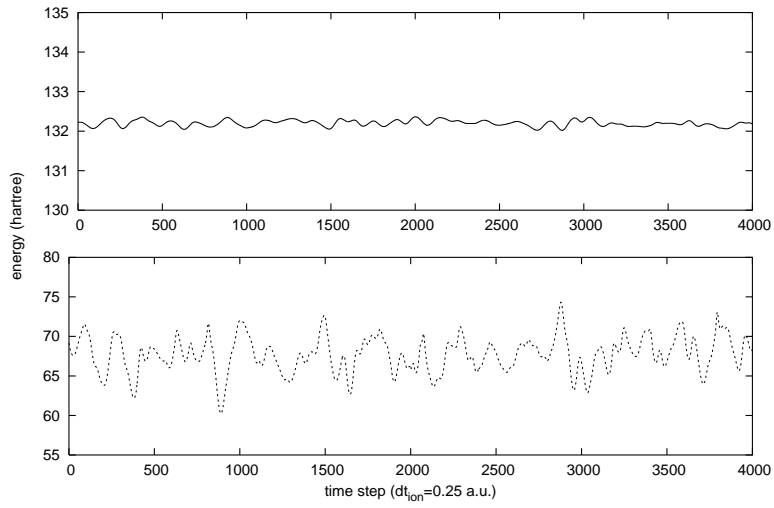


FIG. 2: Total (solid line) and potential (dotted line) energies corresponding to the simulation of {63 H, 1 He} with the switching parameter equal to 0.5.

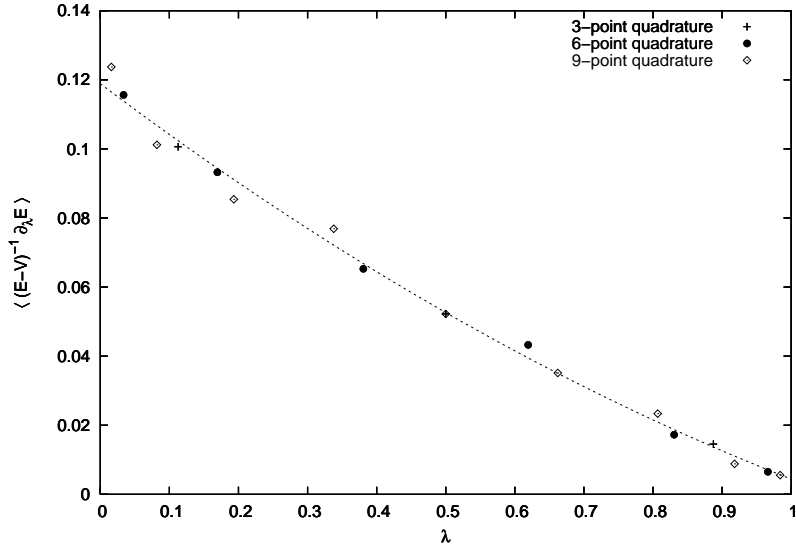


FIG. 3: Different values of  $\left\langle \frac{1}{E(\lambda)-V} \frac{\partial E(\lambda)}{\partial \lambda} \right\rangle$  obtained for the different quadratures. A quadratic fit of the results is given as a guide for the eye.